Journal of Photochemistry & Photobiology, B: Biology 213 (2020) 112074

Contents lists available at ScienceDirect

Journal of Photochemistry & Photobiology, B: Biology

journal homepage: www.elsevier.com/locate/jphotobiol

Elevated CO_2 concentration alleviates UVR-induced inhibition of photosynthetic light reactions and growth in an intertidal red macroalga

Di Zhang [a], Juntian Xu [b], Menglin Bao [b], Dong Yan [a], Sven Beer [c], John Beardall [a,d], Kunshan Gao [a,b,*]

[a] State Key Laboratory of Marine Environmental Science & College of Ocean and Earth Sciences, Xiamen University, Xiamen 361105, China
[b] Co-Innovation Center of Jiangsu Marine Bio-industry Technology, Jiangsu Ocean University, Lianyungang 222005, China
[c] Department of Plant Sciences and Food Security, Faculty of Life Sciences, Tel Aviv University, Tel Aviv 69978, Israel
[d] School of Biological Sciences, Monash University, Clayton, VIC 3800, Australia

ARTICLE INFO

Keywords:
Chlorophyll fluorescence
CO_2 enrichment
Pyropia yezoensis
Photosynthetic light reactions
Photosynthetic rates
UV-radiation

ABSTRACT

The commercially important red macroalga *Pyropia* (formerly *Porphyra*) *yezoensis* is, in its natural intertidal environment, subjected to high levels of both photosynthetically active and ultraviolet radiation (PAR and UVR, respectively). In the present work, we investigated the effects of a plausibly increased global CO_2 concentration on quantum yields of photosystems II (PSII) and I (PSI), as well as photosynthetic and growth rates of *P. yezoensis* grown under natural solar irradiance regimes with or without the presence of UV-A and/or UV-B. Our results showed that the high-CO_2 treatment (~1000 μbar, which also caused a drop of 0.3 pH units in the seawater) significantly increased both CO_2 assimilation rates (by 35%) and growth (by 18%), as compared with ambient air of ~400 μbar CO_2. The inhibition of growth by UV-A (by 26%) was reduced to 15% by high-CO_2 concentration, while the inhibition by UV-B remained at ~6% under both CO_2 concentrations. Homologous results were also found for the maximal relative photosynthetic electron transport rates ($rETR_{max}$), the maximum quantum yield of PSII (F_v/F_m), as well as the midday decrease in effective quantum yield of PSII (YII) and concomitant increased non-photochemical quenching (NPQ). A two-way ANOVA analysis showed an interaction between CO_2 concentration and irradiance quality, reflecting that UVR-induced inhibition of both growth and YII were alleviated under the high-CO_2 treatment. Contrary to PSII, the effective quantum yield of PSI (YI) showed higher values under high-CO_2 condition, and was not significantly affected by the presence of UVR, indicating that it was well protected from this radiation. Both the elevated CO_2 concentration and presence of UVR significantly induced UV-absorbing compounds. These results suggest that future increasing CO_2 conditions will be beneficial for photosynthesis and growth of *P. yezoensis* even if UVR should remain at high levels.

1. Introduction

Photosynthetic components within thylakoid membranes, especially those of photosystem II (PSII), have been implicated as being highly affected by stress. While photoinhibitory non-photochemical quenching (NPQ) allows dissipation of excess light energy during high irradiances at midday, the high turnover rate of the D1 protein is an efficient means to repair its potential photodamage [1]. Conversely, the slower repair of photosystem I (PSI) subunits [2,3] implies that this photosystem has to be more effectively protected from photodamage. In linear electron transport, PSII and PSI function in series to generate ATP and NADPH needed for CO_2 to be reduced to carbohydrates via the Calvin cycle. A number of studies have shown that the interactions between PSII and PSI are related to the distribution of excitation energy between them and to the redox state of the electron transport chain [4–7]. The occurrence of PSII photoinhibition limits the electron transport from PSII to PSI, and functions as a mechanism that protects PSI from photodamage [6]. The reaction centers' dynamics were reported to be associated with generation of singlet oxygen [8]; therefore, limitation of electron transfers from PSII would also potentially reduce the generation of reactive oxygen species around PSI reaction centers, thus presumably protecting PSI from oxidative damage also in the present work on the red alga. On

* Corresponding author at: State Key Laboratory of Marine Environmental Science & College of Ocean and Earth Sciences, Xiamen University, Xiamen 361105, China.
E-mail address: ksgao@xmu.edu.cn (K. Gao).

https://doi.org/10.1016/j.jphotobiol.2020.112074
Received 23 June 2020; Received in revised form 19 October 2020; Accepted 26 October 2020
Available online 29 October 2020
1011-1344/© 2020 Elsevier B.V. All rights reserved.

the other hand, a lowered activity of PSI might per se induce an excess reduction of the plastoquinone pool, which functions as an important redox sensor for signalling imbalances between the relative excitation of the two photosystems, aggravating photoinhibition of PSII [9,10]. Photoinhibition of PSI may also decrease the rate of the PSII repair cycle by lowering ATP synthesis, which would further increase the net degree of PSII photodamage. Alternatively, an increase of PSI activity would 1) accelerate the rate of electron transport through PSI [11], 2) enhance cyclic electron transport (CET) around PSI [12], and/or 3) participate in the radiation-less quenching of absorbed light energy [13], thus alleviating photodamage of PSII and maintaining the functional integrity of the photosynthetic apparatus.

Intertidal macroalgae are exposed to more extreme diurnally fluctuating conditions than most other plants [14]. These conditions include exposure to high midday irradiances of both photosynthetically active radiation (PAR, 400–700 nm) and UV radiation (UVR, 280–400 nm) during emergence at low tide. While UVR has been reported to exert either inhibitory or enhanced effects on photosynthesis and growth in both macroalgae and phytoplankton [15–18], high levels of UV-A have specifically been shown to inhibit growth and photosynthesis of the macroalga *Gracilaria lemaneiformis* [19], while moderate levels benefitted the grown of *Fucus gardneri* [20] and *Pyropia haitanensis* [21], as well as some other macroalgal species [19]. Similarly varying results were also observed for phytoplankton, where photosynthetic rates showed a significant enhancement under PAR + UVR on cloudy days, while they decreased on sunny days [22]. These various responses may, however, change in the future along with increasing CO_2 concentrations.

Enrichment of CO_2, and the consequently increased acidity of seawater, have been shown to affect the photosynthetic performance of marine algae by 1) increasing photoinhibition of electron transport, as evidenced by a decrease in the effective quantum yield of PSII (YII) and an increase in NPQ [23], 2) an increase in YII and a decrease in NPQ [24], or 3) not significantly affecting the effective absorption cross-section of PSII, YII, NPQ and the maximum quantum yield of PSII (F_v/F_m) [25–28]. The above, as well as most previous studies of the combined effects of increased CO_2 concentrations and UVR in macroalgae, have merely focused on PSII, without reference to PSI [29, 30 and references therein]. This is probably because, as indicated above, PSII has generally been viewed as being more susceptic to environmental fluctuations and stress than PSI. However, again, PSII and PSI work together to maintain the functional integrity of the photosynthetic apparatus. Here we hypothesized that an elevated concentration of CO_2 could modulate potentially inhibitory effects of high solar radiation (both PAR and UVR) by affecting PSII and PSI differentially. This was tested by exposing the red alga *Pyropia yezoensis*, an economically important macroalgal species growing in the high-irradiance upper intertidal, to an elevated CO_2 concentration and UVR interactively.

2. Materials and Methods

2.1. Experimental Treatments

Thalli of *Pyropia yezoensis* were collected from farmed rafts offshore of Gaogong Island (34°54′31″N, 119°31′57″E), Lianyungang, Jiangsu Province, China, and taken to the laboratory in a cooled Styrofoam box within 2 h. Following rinsing, weighed thalli of ~0.05 g fresh weight (FW) were grown for 9 days in 1 L open-ended quartz tubes filled with natural seawater, which was renewed every 2 days. The tubes were partly immersed in a flow-through water bath, keeping them at the ambient seawater temperature of 8 ± 1 °C and slanted so that the thalli faced the sky at an almost perpendicular angle. The seawater in each tube was continuously sparged with ambient air containing 400 ± 20 μbar CO_2, or 1000 ± 40 μbar CO_2. The higher CO_2 level was obtained using a CO_2 enricher (HP 1000 G-D, Ruihua Instruments, Wuhan, China), which controls the CO_2 concentration with less a than 5% variation. In order to provide irradiances of only photosynthetically active radiation (PAR, 400–700 nm) or PAR with a selected UV-radiation (UVR), the quartz tubes were covered with Ultraphan film 395 (UV Opak, Digefra, Munich, Germany) transmitting PAR, Folex 320 film (Montagefolie, Folex, Dreieich, Germany) transmitting PAR + UV-A (UV-A at 315–400 nm), or Ultraphan film 295 (Digefra) transmitting PAR + UV-A + UV-B (UV-B at 280–315 nm), i.e. full sunlight (as used also by Gao et al. [31]). These filters reduce the irradiance ~10% of non-filtered PAR. All measurements were carried out on three independent replicates.

2.2. Solar Irradiance, Growth, and Carbonate Chemistry Parameters

The incident solar irradiance was continuously recorded by a broadband solar radiometer (EKO Instruments Co., LTD, Japan), which has three channels: for PAR 400–700 nm), UV-A (315–400 nm) and UV-B (280–315 nm).

Relative growth rates (RGR) were determined by measuring the changes in FW of the thalli after 9 days of growth, using the equation $RGR(\%\ d^{-1}) = 100\times(\ln N_t - \ln N_{t-9})/9$, where N_t and N_{t-9} represented fresh weights of the thalli at times t and t-9, respectively. Ultraviolet radiation (UVR)-induced growth inhibition was calculated as $(R_{PAR}-R_{PAR+UVR})/R_{PAR}$x100%, where R_{PAR} and $R_{PAR+UVR}$ represented the RGR under PAR alone or PAR + UVR, respectively. The difference between UVR- and UV-A-induced inhibition was used to evaluate the inhibition of UV-B.

The pH_{NBS} was measured at the end of each day by a pH meter (pH 700, Eutech Instruments, Singapore) equipped with an Orion® 8102BN Ross combination electrode (Thermo Electron Co., USA) calibrated with NBS standard buffers (Thermo Fisher Scientific Inc., USA). Total alkalinity (TA) was measured with a TA analyzer (AS-ALK1, Apollo SciTech, USA) by Gran acidimetric titrations. The value of pH_{total} and other carbonate chemistry parameters (e.g. total inorganic carbon concentration, TIC, including bicarbonate and carbonate ions), were calculated by the Excel program CO2SYS [32] according to the measured values of TA and pH_{NBS}.

2.3. Measurements and Analyses of Gas Exchange and Chlorophyll Fluorescence

A GFS-3000 gas exchange system (Walz, Effeltrich, Germany) was used to measure net CO_2 assimilation rates (CAR, mmol CO_2 g^{-1} FW h^{-1}), which were automatically calculated according to von Caemmerer and Farquhar [33]. The external aerial CO_2 concentrations were 400 and 1000 μbar for low-CO_2 and high-CO_2 treatments, respectively. The relative air humidity and the red actinic light were 80% and 200 μmol photons m^{-2} s^{-1}, respectively. Although growth rates were measured here under submergence, photosynthesis progressed in air as well, as was also previously shown for another *Pyropia* sp. [34].

A dual-wavelength pulse-amplitude modulated (PAM) fluorescence monitoring system (Dual-PAM-100, Walz, Effeltrich, Germany) was employed to simultaneously measure photosystem II (PSII) and photosystem I (PSI) quantum yields (YII and YI, respectively) as described by Klughammer and Schreiber [35,36]. The minimal fluorescence (F_o) for 20 min dark-adapted thalli was induced by a pulsed red measuring light of low irradiance (~8 μmol photons m^{-2} s^{-1}), and the maximum fluorescence (F_m) was measured during a 0.8 s saturating flash (~10,000 μmol photons m^{-2} s^{-1}). The $P700^+$ signal measured with the dual-wavelength (830/875 nm) unit of the instrument was taken as the redox state of P700. After 10 s exposure to far-red light, a saturation flash was applied to determine the maximum $P700^+$ signal (P_m). The steady-state fluorescence (F) and $P700^+$ signal (P) were monitored periodically under actinic (photosynthesis-stimulating) light generated by the instrument at the same irradiance as the natural sunlight. The 0.8 s saturating flash was applied to induce the maximum fluorescence (F_m') and maximum $P700^+$ value (P_m'). The maximum quantum yield of PSII (F_v/F_m) and the effective quantum yields of PSII (YII) and PSI (YI) were calculated as (F_m-F_0)/Fm, (F_m'-F)/Fm' and (P_m'-P)/P_m, respectively

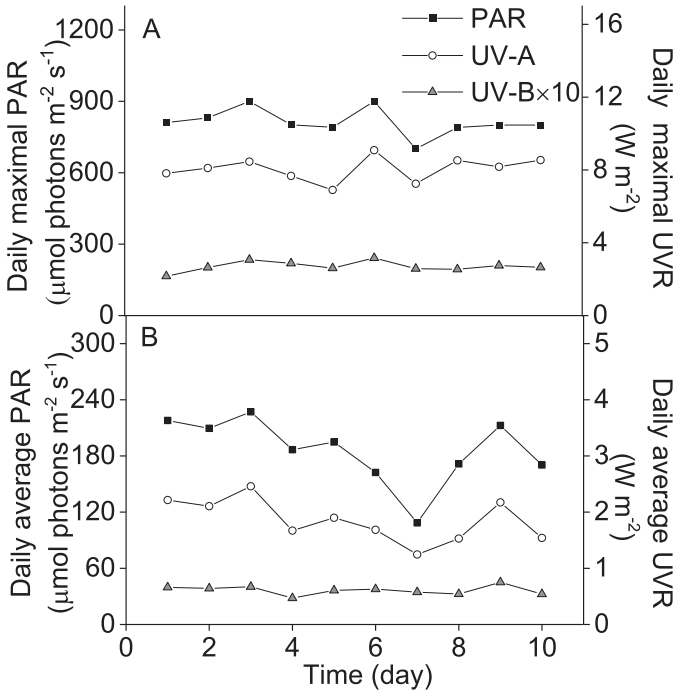

Fig. 1. Daily maximal (A) and daily average (B) irradiances of photosynthetically active radiation (PAR, 400–700 nm, black squares), UV-A (315–400 nm, open circles) and UV-B × 10 (280–315 nm, grey triangles) for the 10 days of incubation.

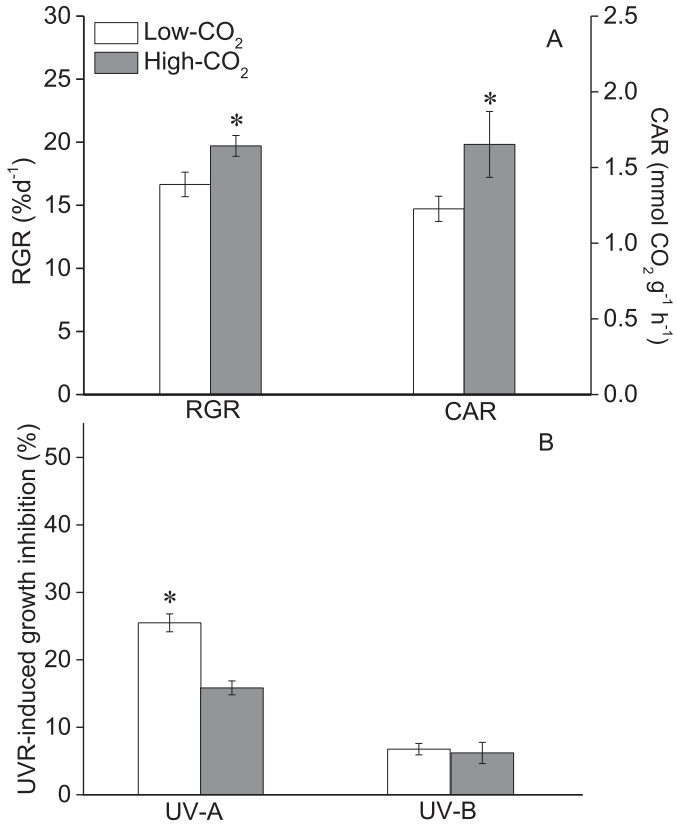

Fig. 2. Relative growth rates (RGR, % d^{-1}), net CO_2 assimilation rates (CAR, mmol CO_2 g^{-1} FW h^{-1}, panel A) and UVR-induced inhibition of growth (%, panel B) of *Pyropia yezoensis* after growing for 9 days at low (~400 μbar, open bars) and high (~1000 μbar, grey bars) CO_2 concentrations. Each data point is the mean ± SD (n = 3). The symbol * indicates significant differences between the treatments in each staple-pair, $p < 0.05$ (t-tests).

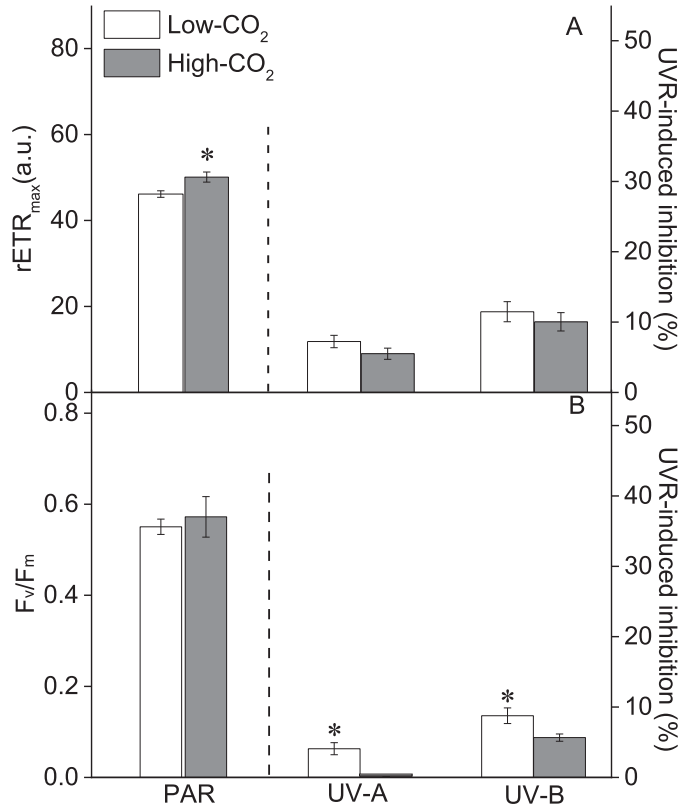

Fig. 3. Values (a.u., left staple-pair) and UVR-induced inhibition (%, right two staple-pairs) on the maximum relative electron transport rates ($rETR_{max}$, panel A) and the maximum yields of PSII (F_v/F_m, panel B) of *Pyropia yezoensis* after growing for 9 days at low (~400 μbar, open bars) and high (~1000 μbar, closed bars) CO_2 conditions. Each data point is the mean ± SD (n = 3). The symbols * indicate significant difference between treatments in each staple-pair, $p < 0.05$ (t-tests).

[35]. Non-photochemical quenching (NPQ) was calculated as NPQ = (F_m-F_m')/Fm'.

Thalli were illuminated for 20 s with 11 incremental steps of increasing actinic irradiance to obtain rapid light curves (RLCs). A saturation flash was applied following each irradiance to generate corresponding F and Fm' values. Relative electron transport rates (rETR) were calculated as (F_m'-F)/Fm'(=YII) × PAR where PAR is the incident photosynthetically active radiation. Maximal ETRs (ETR_{max}) were obtained from these RLCs. Similarly, UVR-induced inhibition were calculated as (P_{PAR}-$P_{PAR+UVR}$)/P_{PAR}x100%, where P_{PAR} and $P_{PAR+UVR}$ represented the different parameters under PAR alone or PAR + UVR, respectively. UV-B induced inhibition were estimated as the difference between parameters under PAR + UV-A + UV-B and PAR + UV-A.

2.4. Determination of UV-Absorbing Compounds (UVACs)

About 0.1 g (FW) thalli was ground and extracted in 10 ml absolute methanol at 4 °C in darkness for 24 h. After centrifugation at 5000*g* for 15 min, absorbance of the supernatant was measured from 200 to 800 nm using a scanning spectrophotometer (Lamda 35, Perkin Elmer, USA); the absorptivity of UVACs were obtained based on their absorption peak at 340 nm [37].

2.5. Statistical Analyses

Statistical analyses were performed using SPSS 19.0 (SPSS Inc., Chicago, USA). The homogeneity of variance was examined using Levene's test before all statistical analyses. One-way ANOVA and *t*-tests were used to establish differences among treatments. A two-way ANOVA was used to test the interactions on the relative growth rate (RGR) and the effective quantum yields of PSII (YII) and PSI (YI). Differences were considered to be significant at $p < 0.05$.

3. Results

3.1. Water Chemistry and Solar Irradiances

The enhanced CO_2 level (from ~400 to ~1000 μbar in the air phase) resulted an average pH drop from 8.24 ± 0.03 to 7.92 ± 0.03 ($n = 27$). While total alkalinity (TA) remained unaltered, the total inorganic carbon concentration (TIC) increased from 2131 ± 20 to 2310 ± 20 μM and that of CO_2 from 12 ± 1 to 28 ± 3 μM (n = 27) under the high-CO_2 treatment.

The maximal and daily photosynthetically active radiation (PAR) and UV radiation for the 10 days of sun exposure are shown in Fig. 1A and B, respectively. The maximal and daily average PAR during this time period were 812.6 ± 57.4 and 186.1 ± 35.1 μmol photons m^{-2} s^{-1}, respectively, while the corresponding values for UV-A were 8.1 ± 0.7 and 1.9 ± 0.3 W m^{-2}, and 0.3 ± 0.03 and 0.1 ± 0.01 W m^{-2} for UV-B. At noon of the 10th day (when the following measurements were made), PAR, UV-A and UV-B levels were 823 μmol photons m^{-2} s^{-1} and 9.6 and 0.4 W m^{-2}, respectively.

3.2. Growth, Photosynthetic Performances and UV Absorptivity

Both the relative growth rates (RGR) and CO_2 assimilation rates (CAR) of *P. yezoensis* were enhanced by the CO_2 enrichment under the PAR-only treatment (Fig. 2A, t-test, $p < 0.05$, $p < 0.05$). However, UVR significantly reduced RGR at both CO_2 concentrations (Fig. 2B, t-test, $p < 0.05$, $p < 0.05$), there was a 25.5% and 15.8% growth reduction by UV-An under normal- and high-CO_2 conditions, respectively, while UV-B inhibited growth by only 6.3% and 6.5% under those same CO_2 levels (Fig. 2B). No significant difference was observed in RGR between the two CO_2 concentrations under PAR + UVR (i.e. including both UV-A and UV-B, *t*-test, $p = 0.726$).

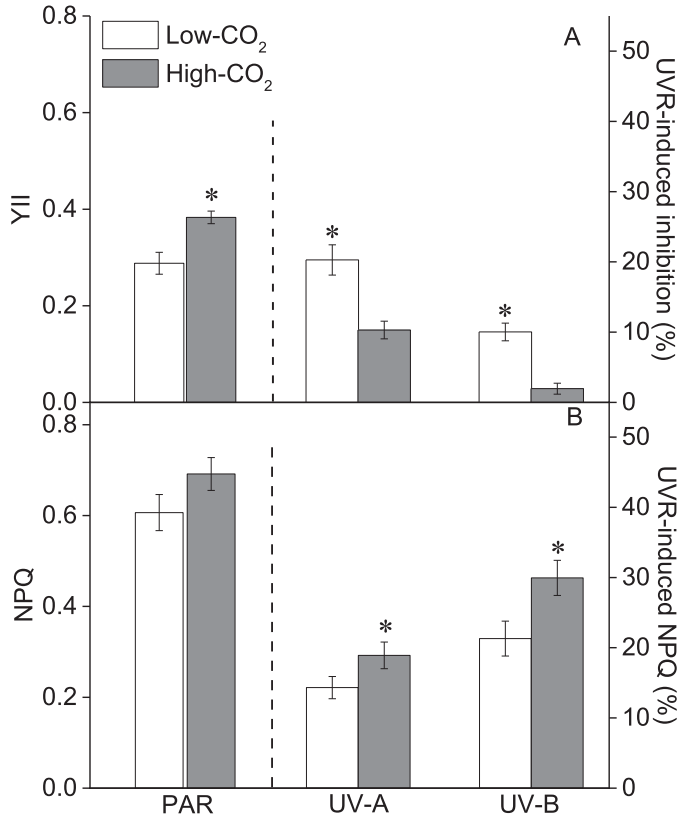

Fig. 4. Values (left staple-pairs) and UVR-induced inhibition (%, right two staple-pairs) of the effective quantum yield of PSII (YII, panel A) and the non-photochemical quenching (NPQ, panel B), of *Pyropia yezoensis* at noon time after growing for 9 days at low (~400 μbar, open bars) and high (~1000 μbar, closed bars) CO_2 conditions. Each data point is the mean ± SD (n = 3). The symbols * indicate significant difference between the treatments in each staple-pair, $p < 0.05$ (t-tests).

Similarly to RGR, the relative maximum rate of electron transfer through PSII ($rETR_{max}$), increased as a result of CO_2 enrichment (*t*-test, $p < 0.05$), but decreased significantly with the addition of UVR (t-test, $p < 0.05$, $p < 0.05$). The UV-A induced inhibitions were 7.2% and 5.5%, while UV-B induced inhibition values were 10.5% and 11.8%, under low- or high-CO_2, respectively. Again, no significant difference was found between the two CO_2 concentrations under the PAR + UVR treatment (Fig. 3A, t-test, $p = 0.459$). Regarding the maximal quantum yield of PSII (F_v/F_m), there was no difference between ambient- and high-CO_2 treatments under PAR-only radiation (t-test, $p = 0.625$), but the high CO_2 treatment did lead to a lower inhibition of F_v/F_m in the presence of UVR (Fig. 3B). Furthermore, the inhibition induced by UV-B treatments was higher than that of UV-A.

During the course of exposure, the effective quantum yields of PSII (YII) showed significant decrease at noon of the 10th day, and there was a higher value of YII in the high CO_2-grown thalli. The presence of UV-A and UV-B significantly inhibited the efficiency of PSII, as reflected in the decrease of YII (*t*-test, $p < 0.05$, $p < 0.05$). Similarly, UV induced inhibition was lower under the high CO_2 conditions, with values of 20.3% (UV-A), 10.3% (UV-B) in low-CO_2 treatments and 10.0% (UV-A), 2.0%

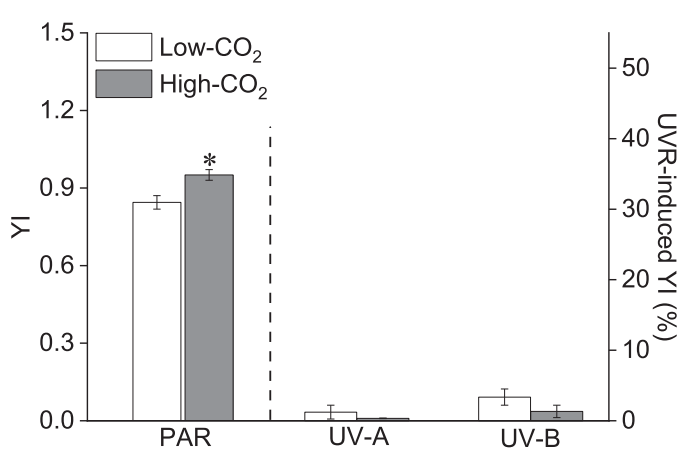

Fig. 5. Values (lef staple-pair) and UVR-induced inhibition (%, left two staple-pairs) of the effective quantum yield of PSI (YI) of *Pyropia yezoensis* at noon time after growing for 9 days at low (~400 μbar, open bars) and high ~(1000 μbar, closed bars) CO_2 conditions. Each data point is the mean ± SD (n = 3). The symbols * indicate significant difference between the treatments in each staple-pair, $p < 0.05$ (t-tests).

Table 1
Two-way ANOVA for the effects of CO_2 (~400 and ~ 1000 μbar) and irradiance quality (PAR, PAR + UV-A and PAR + UV-A + UV-B) on the relative growth rate (RGR) and the effective quantum yields of PSII (YII) and PSI (YI).

Parameters	Source of variation	df	Mean square	F	p
RGR	CO_2	1	34.942	34.649	<0.001
	Irradiance quality	2	46.360	45.971	<0.001
	CO_2× Irradiance quality	2	21.233	21.055	<0.001
	Error	12	1.008		
YII	CO_2	1	0.013	39.350	<0.001
	Irradiance quality	2	0.004	12.086	0.001
	CO_2× Irradiance quality	2	0.003	9.076	0.004
	Error	12	<0.001		
YI	CO_2	1	0.066	117.308	<0.001
	Irradiance quality	2	0.001	1.786	0.209
	CO_2× Irradiance quality	2	<0.001	0.715	0.509
	Error	12	0.001		

(UV-B) in high-CO_2-grown thalli, respectively (Fig. 4A).

Midday non-photochemical quenching (NPQ) values increased as a function of radiation in all treatments. Under PAR only, there was no significant difference in NPQ between the low- and high-CO_2 treatments (*t*-test, $p = 0.208$). With the addition of UVR, NPQ increased significantly, especially in the presence of UV-B. The increases in NPQ were 16.3% under UV-A and 21.3% under UV-B in the low-CO_2 treatments, and 14.9% under UV-A and 29.4% under UV-B in high-CO_2 treatments (Fig. 4B).

The effective quantum yield of PSI (YI) under PAR only showed a significantly higher value under the high-CO_2 treatments at noon of the 10th day of incubation (*t*-test, $p < 0.05$). However, there was no significant difference with the addition of UVR (Fig. 5, *t*-test, $p = 0.489$ for UVA, $p = 0.237$ for UV-B).

A two-way ANOVA showed that both CO_2 level and irradiance quality, and their interaction, significantly affected RGR and the performance of PSII (t-test, $p < 0.05$, $p < 0.05$, $p < 0.05$), while their interaction did not bring significant changes to that of PSI, where only the CO_2 concentration significantly enhanced YI (Table 1, t-test, $p < 0.05$).

As shown in Fig. 6, the presence of UVR brought about significant increase in UV–absorbing compounds (UVAC) (t-test, $p < 0.05$, $p < 0.05$), as quantified by 22.6% by UV-A and 6.4% by UV-B in low-CO_2-grown thalli, and 25.3% by UV-A, and 10.0% by UV-B in high-CO_2-grown thalli. Under PAR only, the CO_2 enrichment increased the absorptivity of UVACs by 8.9%.

4. Discussion

In the present study, both relative electron transport rates ($rETR_{max}$) and net CO_2 assimilation rates (CAR) of *Pyropia yezoensis* showed higher values when grown in sunlight under high-CO_2 conditions, leading to the parallel enhancement of its relative growth rate (RGR). The high-CO_2 treatment (2.5 times ambient values) brought about a 2.3-fold increase in the dissolved CO_2 concentration, while the total dissolved inorganic carbon (TIC) increased only some 8%, due to the reduced pH. The increased CO_2 availability apparently enhanced the carboxylation rate of Rubisco, which is often considered a bottleneck for achieving maximal photosynthetic rates [38–40]. In addition, elevated CO_2 concentrations would also likely increase the CO_2/O_2 ratio around Rubisco, thus accelerating photosynthetic CO_2 fixation [41]. On the other hand, both photosynthesis and growth were significantly inhibited by the presence of UV radiation (UVR). This is similar to other macroalgae, where growth and photosynthetic capacity and efficiency showed lower values under PAR + UVR (Quesada et al. [42] for a mat-forming cyanobacterium; Han and Han [17] for *Ulva pertusa*; [43] and references therein; [44]). The strong correlation between photosynthesis and growth indicates that both midday net CAR and $rETR_{max}$ could be used as a proxy to indicate the effects of both UVR and CO_2 on growth responses for macroalgae such *as P. yezoensis*. Two-way ANOVA results confirmed that there was an interaction between CO_2 and irradiance quality, and UVR-induced inhibition of both RGR and $rETR_{max}$ were alleviated under the high-CO_2 concentration. Similar results were also found for several microalgae [45,46] and the red macroalga *Gracilaria lemaneiformis* [19].

The maximum quantum yield of PSII (F_v/F_m) showed no significant difference between low- and high-CO_2 treatments, but decreased with the addition of UVR. Moreover, UVR induced less inhibition in the high CO_2-grown thalli, showing an alleviation of PSII photoinhibition by increasing CO_2 availability. Similar results were also found in species of *Ulva* [47–49]. A plausible explanation for this is that the enhancement of CO_2 assimilation rate led to a larger electron sink, thus alleviating the reduction-pressure on the photosystems. However, in some calcifying microalgae, the high-CO_2 would hamper the calcification in coccolithophorids, consequently thinning calcified layer and allowing more transmission of UV, thus exacerbating the damage induced by UVR and impairing cellular functions [50–52].

As reviewed by Villafañe et al. [16], UVR inhibited photosynthesis of both micro- and macro-algae by direct impacts through 1) pigment photobleaching in the photosynthetic antenna, 2) reduction of proteins

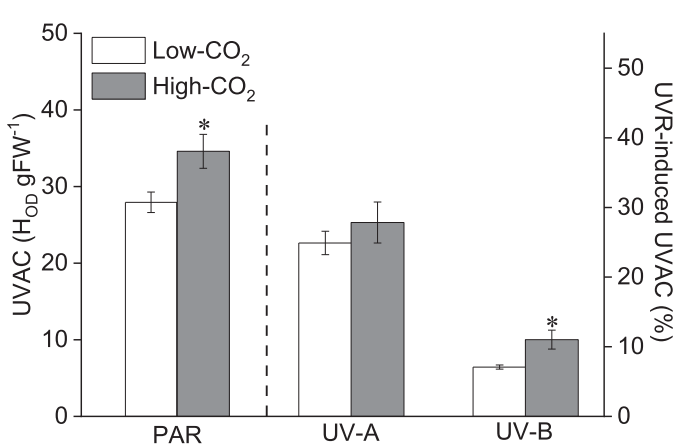

Fig. 6. Values (H_{OD} gFW^{-1}, left staple-pair) and UVR-induced reduction (%, right stapele-pairs) of UV-absorbing compounds (UVAC) of *Pyropia yezoensis* at noon time after growing for 9 days at low (~400 μbar, open bars) and high (~1000 μbar, grey bars) CO_2 conditions. Each data point is the mean ± SD (n = 3). The symbols * indicate significant difference between the treatments in each staple-pair, $p < 0.05$ (t-tests).

in PSII, 3) decrease of enzyme activity in the Calvin cycle, and 4) inhibition of carbonic anhydrase activity, as well as via indirect effects such as DNA damage. In the present study, measurements of the effective quantum yields of PSII (YII) showed that *P. yezoensis* suffered significant photoinhibition in the prescence of UVR, which most probably related to the degradation of the D1 protein. However, the inhibition by UV-A and, especially, UV-B was lessened with the enrichment of CO_2. Even in the PAR-alone condition, YII showed a higher value under the high-CO_2 treatment. The antagonistic effect between CO_2 and irradiance was also verified by the two-way ANOVA analysis. In a previous study, the enrichment of CO_2 down-regulated the function of the CO_2 concentrating mechanism in *P. yezoensis* [29], the energy requirement of which could be diverted toward processes such as repair of the D1 protein. This would thus increase the resilience of PSII to both high PAR and UVR, and may be the reason for the non-photochemical quenching (NPQ) showing insignificant differences here between low- and high-CO_2 treatments under PAR alone condition.

NPQ plays an important role in regulating the distribution of excitation energy between PSII and PSI. As reported in red tide alga *Phaeocystis globosa*, combined effects of elevated CO_2 and UV-A varied with intensities of the irradiances, as characterized by an increasing/decreasing NPQ under sunny/cloudy days, respectively [53]. However, the interaction between UV-B and high-CO_2 concentration always increased NPQ [53], which is consistent with the results in the present work (Fig. 4B). In this study, NPQ increased with the addition of UVR (especially for UV-B) as well as with the CO_2 enrichment. The increase of NPQ could be attributed to alleviating UVR-related damage and possible seawater-acidification stress associated with high CO_2 conditions. Such enhanced non-photochemical performance appeared to result in increased PSII resilience to UVR and the combination of UVR and CO_2.

As shown in the present work, both UV-A and UV-B damaged PSI to a much lesser exent than PSII in the red alga, *P. yezoensis*. This is consistent with previous works on both terrestrial plants and other marine microalgae [54–57]. Unlike for YII, we actually found a slight, albeit statistically non-significant, increase in YI as the daily irradiance increased toward noon (results not presented), suggesting that PSI was more protected against photoinhibition. This may relate to the lowered electron transport from PSII, which would keep PSI from over-reduction [3] and avoid the generation of ROS [8]. A two-way ANOVA analysis showed that CO_2 enrichment resulted in a higher level of YI, but UV radiation and the interaction showed no significant effects.

The synthesise UV-absorbing compounds (UVACs) in some macroalgae have been reported to function: 1) as "nature's sunscreen compounds", absorbing the high-energy photons and dissipating the energy as heat; 2) as antioxidant molecules, scavenging reactive oxygen species, thus protecting thalli from photoinhibition/photodamage and coping with the fluctuation of UV radiation [58]. In the present study, concentrations of UVACs increased significantly in the presence of UV-A and UV-B radiation. Similar results were also observed in red macroalgae *Gracilaria lemaneiformis* [59], *Pyropia haitanensis* [60], as well as the green macroalga *Ulva pertusa* [17]. UVR-induced UVACs showed higher values in the high CO_2-grown thalli; therefore the elevated CO_2 did enhance the protection of *P. yezoensis* against UVR.

The red alga *P. yezoensis* is in nature exposed to high solar UVR in the upper intertidal (where it even grows part-time as an emergent), which harms its photosynthetic performance. However, as shown here, such a negative impact will be largely counteracted by increasing availability of CO_2 in the future. Our data imply that such elevated CO_2 levels could increase quantum efficiencies of both PSII and PSI in concert with CO_2 assimiation rates and, consequently, enhance its growth even in the presence of potentially high levels of UVR.

Declaration of Competing Interest

The authors declared that they have no conflict, informed consent, or animal rights applicable in publishing this article. The authors declared that they have no conflicts of interest.

Acknowledgments

This study was supported by the National Natural Science Foundation (41720104005, 41721005). We are grateful to Xianglan Zeng and Wenyan Zhao for their technical assistance.

References

[1] R.L. Burnap, D1 protein processing and Mn cluster assembly in light of the emerging photosystem II structure, Phys. Chem. Chem. Phys. 6 (2004) 4803–4809.
[2] S.B. Powles, Photoinhibition of photosynthesis induced by visible light, Annu. Rev. Plant Physiol. 35 (1984) 15–44.
[3] K. Sonoike, Photoinhibition of photosystem I, Physiol. Plant. 142 (2011) 56–64.
[4] J. Harbinson, C.L. Hedley, The kinetics of $P700^+$ reduction in leaves: a novel in situ probe of thylakoid functioning, Plant Cell Environ. 12 (1989) 357–369.
[5] A. Danon, S.P. Mayfield, Light-regulated translation of chloroplast messenger RNAs through redox potential, Science 266 (1994) 1717–1719.
[6] M. Tikkanen, N.R. Mekala, E.M. Aro, Photosystem II photoinhibition-repair cycle protects photosystem I from irreversible damage, Bioch. Biophys. Acta B 2014 (1837) 210–215.
[7] D. Zhang, Q.S. Zhang, X.Q. Yang, Z.T. Sheng, G.N. Nan, The alternation between PSII and PSI in ivy (*Hedera nepalensis*) demonstrated by in vivo chlorophyll a fluorescence and modulated 820 nm reflection, Plant Physiol. Biochem. 108 (2016) 499–506.
[8] A.F. Uchoa, P.P. Knox, R. Turchielle, N.K. Seifullina, M.S. Baptista, Singlet oxygen generation in the reaction centers of *Rhodobacter sphaeroides*, Eur. Biophys. J. 37 (2008) 843–850.
[9] P. Haldimann, M. Tsimilli-Michael, Mercury inhibits the non-photochemical reduction of plastoquinone by exogenous NADPH and NADH: evidence from measurements of the polyphasic chlorophyll *a* fluorescence rise in spinach chloroplasts, Photosynth. Res. 74 (2002) 37–50.
[10] S.Z. Tóth, G. Schansker, R.J. Strasser, A non-invasive assay of the plastoquinone pool redox state based on the OJIP-transient, Photosynth. Res. 93 (2007) 193.
[11] M. Havaux, F. Tardy, Temperature-dependent adjustment of the thermal stability of photosystem II in vivo: possible involvement of xanthophyll-cycle pigments, Planta 198 (1996) 324–333.
[12] R. Zhang, T.D. Sharkey, Photosynthetic electron transport and proton flux under moderate heat stress, Photosynth. Res. 100 (2009) 29–43.
[13] H. Pettai, V. Oja, A. Freiberg, A. Laisk, The long-wavelength limit of plant photosynthesis, FEBS Lett. 579 (2005) 4017–4019.
[14] J.J. Bolton, What is aquatic botany? And why algae are plants: the importance of non-taxonomic terms for groups of organisms, Aquat. Bot. 132 (2016) 1–4.
[15] T. Han, Y.S. Han, J.M. Kain, D.P. Häder, Thallus differentiation of photosynthesis, growth, reproduction, and UV-B sensitivity in the green alga *Ulva pertusa* (Chlorophyceae), J. Phycol. 39 (2003) 712–721.
[16] V.E. Villafañe, K. Sundbäck, F.L. Figueroa, E.W. Helbling, Photosynthesis in the aquatic environment as affected by UVR, in: UV Effects in Aquatic Organisms and Ecosystems, The Royal Society of Chemistry, Cambridge, 2003, pp. 357–397.
[17] Y.S. Han, T. Han, UV-B induction of UV-B protection in *Ulva pertusa* (Chlorophyta), J. Phycol. 41 (2005) 523–530.
[18] M.V.F. Giordanino, S.M. Strauch, V.E. Villafañe, E.W. Helbling, Influence of temperature and UVR on photosynthesis and morphology of four species of cyanobacteria, J. Photochem. Photobiol. B 103 (2011) 68–77.
[19] J. Xu, K. Gao, Use of UV-A energy for photosynthesis in the red macroalga *Gracilaria lemaneiformis*, Photochem. Photobiol. 86 (2010) 580–585.
[20] B.E. Henry, K.L. Van Alstyne, Effects of UV radiation on growth and phlorotannins in *Fucus gardneri* (Phaeophyceae) juveniles and embryos, J. Phycol. 40 (2004) 527–533.
[21] H. Jiang, K. Gao, E.W. Helbling, Effects of solar UV radiation on germination of conchospores and morphogenesis of sporelings in *Porphyra haitanensis* (Rhodophyta), Mar. Biol. 151 (2007) 1751–1759.
[22] K. Gao, Y. Wu, G. Li, H. Wu, V.E. Villafane, E.W. Helbling, Solar UV radiation drives CO_2 fixation in marine phytoplankton: a double-edged sword, Plant Physiol. 144 (2007) 54–59.
[23] Y. Wu, K. Gao, U. Riebesell, CO_2-induced seawater acidification affects physiological performance of the marine diatom *Phaeodactylum tricornutum*, Biogeosciences 7 (2010) 2915–2923.
[24] S. Chen, J. Beardall, K. Gao, A red tide alga grown under ocean acidification upregulates its tolerance to lower pH by increasing its photophysiological functions, Biogeosciences 11 (2014) 4829–4837.
[25] G. Yang, K. Gao, Physiological responses of the marine diatom *Thalassiosira pseudonana* to increased pCO_2 and seawater acidity, Mar. Environ. Res. 79 (2012) 142–151.
[26] C.B. Wall, T.Y. Fan, P.J. Edmunds, Ocean acidification has no effect on thermal bleaching in the coral *Seriatopora caliendrum*, Coral Reefs 33 (2014) 119–130.
[27] C.J. Hoppe, L.M. Holtz, S. Trimborn, B. Rost, Ocean acidification decreases the light-use efficiency in an Antarctic diatom under dynamic but not constant light, New Phytol. 207 (2015) 159–171.
[28] S. Trimborn, S. Thoms, T. Brenneis, J.P. Heiden, S. Beszteri, K. Bischof, Two Southern Ocean diatoms are more sensitive to ocean acidification and changes in

irradiance than the prymnesiophyte *Phaeocystis antarctica*, Physiol. Plant. 160 (2017) 155–170.
[29] X. Li, J. Xu, P. He, Comparative research on inorganic carbon acquisition by the macroalgae *Ulva prolifera* (Chlorophyta) and *Pyropia yezoensis* (Rhodophyta), J. Appl. Phycol. 28 (2016) 491–497.
[30] Y. Ji, Z. Xu, D. Zou, K. Gao, Ecophysiological responses of marine macroalgae to climate change factors, J. Appl. Phycol. 28 (2016) 2953–2967.
[31] K. Gao, H. Yu, M.T. Brown, Solar PAR and UV radiation affects the physiology and morphology of the cyanobacterium *Anabaena* sp. PCC 7120, J. Photochem. Photobiol. B 89 (2007) 117–124.
[32] D. Pierrot, E. Lewis, D.W.R. Wallace, MS Excel program developed for CO_2 system calculations, in: ORNL/CDIAC-105a, Carbon Dioxide Information Analysis Center, Oak Ridge National Laboratory, U.S. Department of Energy, Oak Ridge, TN, 2006.
[33] S.V. Von Caemmerer, G.D. Farquhar, Some relationships between the biochemistry of photosynthesis and the gas exchange of leaves, Planta 153 (1981) 376–387.
[34] Y. Lipkin, S. Beer, A. Eshel, The ability of *Porphyra* lineari (Rhodophyta) to tolerate prolonged periods of desiccation, Bot. Mar. 36 (1993) 517–523.
[35] C. Klughammer, U. Schreiber, An improved method, using saturating light pulses, for the determination of photosystem I quantum yield via $P700^+$-absorbance changes at 830 nm, Planta. 192 (1994) 261–268.
[36] C. Klughammer, U. Schreiber, Complementary PS II quantum yields calculated from simple fluorescence parameters measured by PAM fluorometry and the saturation pulse method, PAM Application Notes 1 (2008) 201–247. http://www.walz.com.
[37] E.W. Helbling, E.S. Barbieri, R.P. Sinha, V.E. Villafane, D.P. Häder, Dynamics of potentially protective compounds in Rhodophyta species from Patagonia (Argentina) exposed to solar radiation, J. Photochem. Photobiol. B 75 (2004) 63–71.
[38] W.J. Campbell, L.H. Allen, G. Bowes, Effects of CO_2 concentration on rubisco activity, amount, and photosynthesis in soybean leaves, Plant Physiol. 88 (1988) 1310–1316.
[39] G. Bowes, Growth at elevated CO_2: photosynthetic responses mediated through Rubisco, Plant Cell Environ. 14 (1991) 795–806.
[40] J.L. Losh, J.N. Young, F.M. Morel, Rubisco is a small fraction of total protein in marine phytoplankton, New Phytol. 198 (2013) 52–58.
[41] H. Wu, D. Zou, K. Gao, Impacts of increased atmospheric CO_2 concentration on photosynthesis and growth of micro-and macro-algae, Sci. China Ser. C 51 (2008) 1144–1150.
[42] A. Quesada, J.L. Mouget, W.F. Vincent, Growth of Antarctic cyanobacteria under Ultraviolet radiation: UVA counteracts UVB inhibition, J. Phycol. 31 (1995) 242–248.
[43] D.-P. Häder, Adaptation to UV stress in algae, in: L.C. Rai, J.P. Gaur (Eds.), Algal Adaptation to Environmental Stresses, Springer, Berlin, 2001, pp. 221–236.
[44] R.P. Sinha, M. Klisch, A. Gröniger, D.-P. Häder, Responses of aquatic algae and cyanobacteria to solar UV-B, Plant Ecol. 154 (2001) 221–236.
[45] Y. Wu, D.A. Campbell, K. Gao, Faster recovery of a diatom from UV damage under ocean acidification, J. Photochem. Photobiol. B 140 (2014) 249–254.
[46] J.J. Valenzuela, A.L.G. de Lomana, A. Lee, E.V. Armbrust, M.V. Orellana, N. S. Baliga, Ocean acidification conditions increase resilience of marine diatoms, Nat. Comm. 9 (2018) 2328.
[47] J. Xu, K. Gao, Future CO_2-induced ocean acidification mediates the physiological performance of a green tide alga, Plant Physiol. 160 (2012) 1762–1769.
[48] M. Olischläger, I. Bartsch, L. Gutow, C. Wiencke, Effects of ocean acidification on growth and physiology of *Ulva lactuca* (Chlorophyta) in a rockpool-scenario, Phycol. Res. 61 (2013) 180–190.
[49] F. Yue, G. Gao, J. Ma, H. Wu, X. Li, J. Xu, Future CO_2-induced seawater acidification mediates the physiological performance of a green alga *Ulva linza* in different photoperiods, PeerJ 7 (2019), e7048.
[50] K. Gao, Z. Ruan, V.E. Villafane, J.P. Gattuso, E.W. Helbling, Ocean acidification exacerbates the effect of UV radiation on the calcifying phytoplankter *Emiliania huxleyi*, Limnol. Oceanogr. 54 (2009) 1855–1862.
[51] K. Xu, K. Gao, Solar UV irradiances modulate effects of ocean acidification on the coccolithophorid *Emiliania huxleyi*, Photochem. Photobiol. 91 (2015) 92–101.
[52] K. Gao, D.P. Häder, Photosynthetic performances of marine microalgae under influences of rising CO_2 and solar UV radiation, in: Q. Wang (Ed.), Microbial Photosynthesis, Springer, Singapore, 2020, pp. 139–150.
[53] S. Chen, K. Gao, Solar ultraviolet radiation and CO_2-induced ocean acidification interacts to influence the photosynthetic performance of the red tide alga *Phaeocystis globosa* (Prymnesiophyceae), Hydrobiologia 675 (2011) 105–117.
[54] Å. Strid, W.S. Chow, J.M. Anderson, Effects of supplementary ultraviolet-B radiation on photosynthesis in *Pisum sativum*, Bioch, Biophys, Acta B 1020 (1990) 260–268.
[55] Å. Strid, W.S. Chow, J.M. Anderson, UV-B damage and protection at the molecular level in plants, Photosynth. Res. 39 (1994) 475–489.
[56] E. Turcsányi, I. Vass, Inhibition of photosynthetic Electron transport by UV-A radiation targets the photosystem II complex, Photochem. Photobiol. 72 (2000) 513–520.
[57] J. Beardall, P. Heraud, S. Roberts, K. Shelly, S. Stojkovic, Effects of UV-B radiation on inorganic carbon acquisition by the marine microalga *Dunaliella tertiolecta* (Chlorophyceae), Phycologia 41 (2002) 268–272.
[58] A. Oren, N. Gunde-Cimerman, Mycosporines and mycosporine-like amino acids: UV protectants or multipurpose secondary metabolites? FEMS Microbiol. Lett. 269 (2007) 1–10.
[59] Y. Zheng, K. Gao, Impacts of solar UV radiation on the photosynthesis, growth, and UV-absorbing compounds in *Gracilaria lemaneiformis* (Rhodophyta) grown at different nitrate concentrations, J. Phycol. 45 (2009) 314–323.
[60] H. Jiang, K. Gao, E. Walter Helbling, The conchocelis of *Porphyra haitanensis* (Rhodophyta) is protected from harmful UV radiation by the covering calcareous matrix, J. Phycol. 45 (2009) 1270–1277.